treatment group. Thus, combining SM-345431 treatment with specific rehabilitation is a reasonable and promising approach to the treatment of SCI.

Other possible mechanisms underlying motor function recovery could include remyelination and angiogenesis. We noticed that, with increases in afferent sensory input, the step lengths of the SM-345431 groups while walking on the treadmill exhibited a linear and gradual improvement throughout the experimental period. The animals treated with SM-345431 showed enhanced remyelination at the lesion site (Figure 4E-J), which could be relevant to a recent study reporting the effects of semaphorin3A on myelination [36]. In general, myelination significantly increases conduction velocity (sometimes up to 100-fold [54]), which results in increased motor function. Thus, remyelination after SM-345431 treatment may have also partially contributed to the enhancement of motor function recovery on the treadmill. Angiogenesis also plays an important role in reducing secondary damage and enhancing tissue repair after SCI, and the extent of angiogenesis correlates with the extent of axon regeneration after SCI [33]. Angiogenesis was significantly enhanced after SM-345431 treatment alone, although combined treatment did not further enhanced this effect statistically (Figure 4A-D). Therefore, angiogenesis may also have contributed to motor function recovery. Interestingly, at the end of the experimental period (3 months post-injury), the incremental effects of the treatment on motor performance, specifically in terms of step height and step cycle area, tended to be more robust in the SM-345431 treatment group than in the combined treatment group (Figure 6D-F). These data indicate that combined treatment may also have expedited motor function recovery and decreased the overall time needed for recovery.

Conclusions

Collectively, our data demonstrate that the administration of SM-345431 via a novel DDS utilizing silicone sheets significantly enhanced axonal regeneration, remyelination and angiogenesis, thereby promoting motor function recovery after SCT in adult rats. Additionally, combining SM-345431 with extensive treadmill training resulted in improved motor function recovery that included continuous plantar step walking on a treadmill with a BSS. This comprehensive effect of combined treatment presumably resulted from the reinforcement of spinal networks in the caudal spinal stump and the rewiring/refinement of regenerated axons. Thus, combining semaphorin3A inhibitor treatment with extensive treadmill training has great potential as a new treatment for SCI. In addition, this study highlights the importance of combining treatments that promote axon regeneration with specific and appropriate rehabilitations that promote rewiring for the effective treatment of SCI.

Methods

Overall experimental outline

Rats were randomly divided into the following three experimental groups: 1) untrained + placebo, 2) untrained + SM-345431 and 3) trained + SM-345431. SCT was performed, and SM-345431 or placebo was administered at the lesion site via the newly developed DDS, which is described in detail below. Starting 1 week post-injury, treadmill training commenced with a BSS. Kinematic tests were performed monthly for 3 months after SCT using a rodent robotic device (Rodent robot 3000, Robomedica Inc.) that primarily assessed the performance of plantar stepping on a treadmill. Treadmill training was continued throughout the experimental period.

Animals and surgical procedures

A total of 53 adult female Sprague-Dawley rats (200-250 g, 10-12 weeks old) were used in this study (3 rats died during the experimental period and were excluded from the statistical analysis). All procedures were approved by the experimental animal care committee of Keio University, School of Medicine and Murayama Medical Center (approval #12-8). All rats were anesthetized with an intraperitoneal injection of ketamine (100 mg/kg)/xylazine (10 mg/kg). The spinal cord at the level of the T10 lamina was exposed by T10 laminectomy, and the dorsal dura mater was opened. The exposed spinal cord was cut along the inner edge of the vertebra with a sharp micro-scissor. Two more cuts were made at the gap of the transected spinal cord by a scalpel to ensure total transection. SM-345431 or placebo was administered to the transected site via the newly developed DDS as described in detail below (Figure 1G-I). After these procedures, the back muscles and skin were closed. Rats were kept warm in an incubator (37°C) after surgery. To prevent dehydration in the rats, 10 ml of saline was subcutaneously injected daily until day 7. Ampicillin (0.4 g/kg) was also injected intramuscularly daily to prevent infection until day 7. The bladder was evacuated manually until autonomous emptying of the bladder was achieved. The re-transection procedure was performed at the same level as the primary SCT (15 rats total; 5 rats from each group). Kinematic data were recorded using similar procedures prior to re-transection surgery (on the same day) and on the day following re-transection surgery. For CST tracing, 10% BDA was injected as follows. Nine weeks after SM-345431 or placebo administration, BDA (10000 MW, Molecular Probes) was injected into six different sites of the sensorimotor cortices of the rats under general anesthesia (site 1: 2.0 mm lateral, 0 mm to bregma; site 2: 2.0 mm lateral, 2 mm posterior to bregma; site 3: 2.0 mm lateral, 4 mm posterior to bregma; site 4: 4 mm lateral, 0 mm to bregma; site 5: 4 mm lateral, 2 mm posterior to bregma and site 6: 4 mm lateral, 4 mm posterior to bregma). For

each site, injections were performed at two different depths (1.2 mm and 1.6 mm), and 3 μl of 10% BDA was injected at a rate of 0.15 μl/min using a micro-injector. Three weeks after the BDA injection, rats were sacrificed and used for immunohistochemistry.

Growth cone collapse assay and collagen co-culture assay

The growth cone collapse assay and collagen co-culture experiments were performed as previously described [20]. To examine the effects of SM-345431-silicone, small pieces (2 × 1 × 0.3 mm; approximately 1 mg containing 1 μg of SM-345431) of the SM-345431-silicone or control-silicone were placed in a collagen gel adjacent to E8 chick DRGs and COS7 cell aggregates, as shown in Figure 1C.

Drug delivery system

A novel matrix silicone preparation was developed to allow continuous drug delivery at the site of injury. The amount of drug released from this matrix silicone preparation *in vitro* was measured as described in Figure 1. Matrix silicone sheets (0.3 mm thick) containing SM-345431 were trimmed into 3-mm-square pieces to fit into the opened dura. After SCT, one piece of silicone sheet was placed on the transected spinal cord gap so that it could act on the spinal cord directly. Silicone sheets of the same size that did not contain SM-345431were used for the control group.

Training protocol

A robotic device (rodent robot 3000, Robomedica Inc.) [55] was used to train the SCT rats. Briefly, the device consisted of a computer-controlled BSS, two lightweight robotic arms and a treadmill with variable motorized speeds. The ankles of the hindlimbs of rats were held with a pair of releasable rope cuffs, which were then secured to robotic arms to track ankle trajectory in the horizontal and vertical directions. A computer-controlled body support arm was used to control the load that was applied to the hindlimbs and to maintain body equilibrium. Rats were secured in a cloth vest and attached to the body support arm with a hook-and-loop fabric. Hard rope cuffs were attached to the hindlimbs of rats with the robotic arm during training.

In our pilot study, we found that it was possible to train spinal cord-transected rats soon after SCT via voluntary walking evoked by sensory input. Additionally, improvements in motor performance were more obvious when the treadmill training was initiated at earlier time points after SCT. Therefore, training was initiated as early as 1 week after SCT. The fixed parameters were set at 50% body weight support (BWS), 20 min/day and 5 days/week. The animals were adapted to the training via increasing velocity; a velocity of 1 cm/s was used in the first week, and then the velocity was increased by 2 cm/s every 2 weeks for the first 2 months after injury (i.e., 1 cm/s to 3 cm/s to 5 cm/s). In the first week of training, rats frequently did not adapt to the acceleration of the treadmill, and this resulted in dragging of the hindlimbs. Once the rats dragged their hindlimbs and stopped walking on the treadmill, a trainer brought their bodies back to the original walking position. The step ability of SCT rats on the treadmill improved gradually over the course of the first 2 months following injury. However, this improvement was attenuated at time points later than 2 months after injury. Hence, at the time points later than 2 months after injury, the velocities of the treadmill were adjusted to 5 to 9 cm/s according to the improvement observed in the hindlimb motion of the rats.

Detailed motor function analysis using kinematics

To evaluate the locomotor capability of SCT rats in detail, the aforementioned robotic device was employed. Each robotic arm tracked the two-dimensional movement of the ankle, and the trajectory of the ankle movement was then recorded on a computer for kinematic analyses. Not all the rats were able to walk by themselves on the treadmill by the last time point of the experiment. Therefore, when performing the tests, the degree of BWS and treadmill speed were titrated to obtain the maximum walking performance on the treadmill. As a result of this titration, the behavioral tests were performed at 70% BWS and a treadmill velocity of 1 cm/s each month after SCT. The duration of testing was 1 min per rat to minimize training effects during testing. The methods of previous reports [44,56] were followed with slight adaptations. Briefly, the ankle trajectory in each plane was recorded by the robotic arm and a computer. Then, the toe off (TO) and paw contact (PC) events in each step cycle were identified using Rodent Robot 3000 software. All kinematic characteristics were obtained when TO and PC were identified; as a result, parameters such as the duration phase, the swing phase of the step cycle and the length and height of the step were calculated. The number of animals used in these behavioral tests was 32 (control: n = 9, SM-345431: n = 12, combined: n = 11).

Immunohistochemistry

Twelve weeks after SCT, rats were deeply anaesthetized by an intraperitoneal injection of 14% chloral hydrate and then perfused intracardially with 4% paraformaldehyde (PFA) in 0.1 M phosphate-buffered saline (PBS). The spinal cord tissues were dissected and post-fixed in 4% PFA (24 h) and placed in 10% sucrose in 0.1 M PBS (24 h) followed by 30% sucrose in 0.1 M PBS (24 h). All the rats other than 3 rats died during the experimental period were used for the histological analysis. Segments of spinal cords were embedded in Optimal Cutting Temperature compound (Tissue Tek) and stored at -80°C. Frozen spinal

cord tissues were cut with a cryostat into 20-μm-thick sections. For diaminobenzidine (DAB) staining, sections were washed with 0.1 M PBS and then presoaked for 30 min in 0.03% H_2O_2 with methanol. After an additional presoak in TNB (0.10 M Tris-HCl, 0.15 M NaCl, 0.5% BMP) for 60 min, sections were incubated at 4°C with rabbit anti-GAP43 (1:300; Millipore), mouse anti-rat RECA-1 (1:500; Serotec) or rabbit polyclonal anti-synapsin-1 (1:300; Chemicon) for 24 h. Subsequently, the sections were washed in 0.1 M PBS and incubated with biotinylated secondary antibodies (1:1,000; Jackson Immunoresearch) for 1 h. Next, the sections were washed and then incubated with an avidin-biotin complex (ABC) (Vectastain Elite ABC Kit, Vector Laboratories) in TNB (1:100) and visualized using DAB (Sigma). Sections were rinsed in PBS, dehydrated using ethanol and xylene and cover-slipped with permount. To identify 5-HT-positive axons that penetrated into the scar tissue area after the treatment, we used a previously described double-staining method [28]. 5-HT was visualized using goat anti-serotonin (5-HT) antibody (1:500; ImmunoStar) and DAB with nickel-glucose oxidase, which produced a black stain. Sections were washed and then incubated with rabbit monoclonal anti-glial fibrillary acidic protein (GFAP; 1:1,000; BD Bioscience Pharmingen) and visualized with DAB, which produced a brown stain. Following these procedures, we identified the range of the scars and quantified the number of 5-HT-positive axons that penetrated into the scar tissue area. To evaluate the status of axonal myelination, immunofluorescent double staining was performed using rabbit anti-GAP43 (1:1,000; Millipore) and rat monoclonal anti-MBP (1:50; Abcam) antibodies. Immunohistochemical analysis for c-Fos in spinal neurons was performed using procedures similar to those previously described [24,41,43]. Briefly, rats were trained using the aforementioned training method of continuous hindlimb bipedal stepping. After 45 min of continuous hindlimb bipedal stepping at 3 cm/s with 50% BWS with a hard nylon rope attachment, rats were allowed a 60-min rest. Subsequently, the rats were anesthetized and perfused intracardially with 4% PFA in PBS. After perfusion, the spinal cords were dissected, post-fixed for 24 h at 4°C and cryoprotected in 30% sucrose in PBS for 3 days. The L1-L5 segments were mounted and frozen, and 20-μm-thick axial sections were cut using a cryostat. All sections were pretreated with 0.03% H_2O_2 and methanol for 30 min and then incubated with rabbit polyclonal anti-c-Fos antibody (1:200; Santa Cruz Biotechnology) for 24 h (at 4°C). Subsequently, the sections were washed in 0.1 M PBS and incubated in biotinylated secondary antibody (1:1,000; goat antibody against rabbit; Jackson ImmunoResearch) for 1 h. The remaining procedures were identical to those performed for DAB staining, as described above. All images were obtained using either an Axioskop 2 Plus microscope (Zeiss) for DAB staining or a LSM510 confocal microscope (Zeiss) for immunofluorescent staining.

Electron microscopic analysis

For electron microscopic analysis, rats from the 3 groups were sampled 72 days after injury. Rats were perfused with 4% PFA in PBS, and the spinal cords were dissected and post-fixed with 2.5% glutaraldehyde overnight at 4°C. After 90 min of fixation with 0.5% osmium tetroxide, the spinal cords were dehydrated with ethanol, acetone and QY1 and then embedded. Ultrathin sections at the epicenter of the lesion sites were prepared at a thickness of 80 nm and stained with uranyl acetate and lead citrate for 15 and 12 min, respectively. The sections were observed with a transmission electron microscope (JEOL model 1230), and images were acquired using Digital Micrograph 3.3 (Gatan Inc.).

Quantitative immunohistochemistry analyses

Immunohistochemical image analyses were performed for all sections of each animal using microscopy, and quantitative analyses were performed by an examiner who was blind to the identities of the animals. Each value is presented as the average value per section (unless otherwise indicated). The number of animals used for quantitative analysis of each staining set ranged from 15 to 21 (5 to 7 animals per group). To quantify the area of GAP-43-positive axons, 5-HT-positive axons and RECA-1-positive vessels, sagittal sections of the spinal cord at the injury site (approximately 1.2 cm in length) were scanned with a CCD camera (DXC-390; Sony). Pictures of the sagittal sections at 1 mm to 3 mm rostral and 1 mm to 3 mm caudal from the injury epicenter were captured for quantitative analyses. The images were analyzed with a Micro Computer Imaging Device (MCID; Imaging Research Inc.). Threshold values were maintained at constant levels for all analyses. 5-HT axons that penetrated into the scar tissue were counted manually. For image analysis, c-Fos-positive (c-Fos+) nuclei from all sections was superimposed onto Molander's cytoarchitectonic maps of the rat thoracic and lumbosacral cord [57]. The expression of synapsin-1 was examined within lamina IX of the L1-L5 segments of the spinal cord using transverse sections and DAB staining. For the quantification of BDA tracing, we followed the methods reported previously [58,59]. The number of CST-positive axons at each distance from the lesion was divided by the number of CST-positive axons at the level of C1 for standardization.

Statistical analyses

For statistical analyses, one-way analyses of variance (one-way ANOVA) and Bonferroni *post hoc* tests were primarily employed to determine significance. Significance was determined using P-values, and the data are presented

as the means ± S.E.M. For the analysis of 5-HT immunostaining, data were analyzed with the Kruskal-Wallis H test. Behavioral data after re-transection were analyzed with t-tests.

Additional file

Additional file 1: Video Representative movies of the *detailed* kinematic *analysis of hindlimb motor performance* on a treadmill at the end of the experimental period. Plantar step walking with a BSS was not observed in control group animals (A). Limited plantar step walking with a BSS was observed in SM-345431 treatment group animals (B). Significantly enhanced plantar step walking with a BSS was observed in the combined treatment group animals. All animals in the combined treatment group continued plantar step walking with a BSS for at least 30 min (C).

Competing interests

H. Okano is a scientific consultant of San Bio, Inc; Eisai Co Ltd; and Daiichi Sankyo Co Ltd.
K. Kikuchi, A. Sano, M. Maeda, A. Kishino and T. Kimura are employed by Dainippon Sumitomo Pharma Co Ltd.

Authors' contributions

LZ and SK performed the experiments and wrote the manuscript. KK, AS, MM, SS, and MM performed the experiments. SK, AK, YT, ML, TK, HO and MM designed the study. All authors read and approved the final manuscript.

Acknowledgments

We thank Kiyokazu Iwata, Toshihiro Nagai and Takahiro Kondo for sample preparation and all members of the Okano laboratory for helpful discussions and support.
This work was supported by grants from the Project for the Realization of Regenerative Medicine from the Ministry of Education, Culture, Sports and Technology (MEXT) of Japan and the Research Center Network for the Realization of Regenerative Medicine to H.O. and M.N.; a grant for young investigators from MEXT to S.K.; a grant from the General Insurance Association of Japan to L.Z., S.K. and M.N. and the Funding Program for World-Leading Innovative R&D on Science and Technology (FIRST Program) to H.O.

Author details

[1]Department of Orthopedic Surgery, Keio University School of Medicine, 35 Shinanomachi, Shinjuku, Tokyo 160-8582, Japan. [2]Department of Physiology, Keio University School of Medicine, 35 Shinanomachi, Shinjuku, Tokyo 160-8582, Japan. [3]Department of Rehabilitation Medicine, Keio University School of Medicine, 35 Shinanomachi, Shinjuku, Tokyo 160-8582, Japan. [4]Department of Orthopedic Surgery, National Hospital Organization, Murayama Medical Center, 2-37-1 Gakuen, Musashimurayama, Tokyo 208-0011, Japan. [5]Dainippon Sumitomo Pharma Co. Ltd., 3-1-98 Kasugade-naka, Konohana-ku, Osaka 554-0022, Japan.

Received: 20 January 2014 Accepted: 12 February 2014
Published: 10 March 2014

References

1. Afshari FT, Kappagantula S, Fawcett JW: **Extrinsic and intrinsic factors controlling axonal regeneration after spinal cord injury.** *Expert Rev Mol Med* 2009, **11**:1–19.
2. Chierzi S, Ratto GM, Verma P, Fawcett JW: **The ability of axons to regenerate their growth cones depends on axonal type and age, and is regulated by calcium, cAMP and ERK.** *Eur J Neurosci* 2005, **21**(8):2051–2062.
3. Davies SJ, Goucher DR, Doller C, Silver J: **Robust regeneration of adult sensory axons in degenerating white matter of the adult rat spinal cord.** *J Neurosci* 1999, **19**(14):5810–5822.
4. Silver J, Miller JH: **Regeneration beyond the glial scar.** *Nat Rev Neurosci* 2004, **5**(2):146–156.
5. Filbin MT: **Myelin-associated inhibitors of axonal regeneration in the adult mammalian CNS.** *Nat Rev Neurosci* 2003, **4**(9):703–713.
6. GrandPre T, Nakamura F, Vartanian T, Strittmatter SM: **Identification of the Nogo inhibitor of axon regeneration as a Reticulon protein.** *Nature* 2000, **403**(6768):439–444.
7. He Z, Koprivica V: **The nogo signaling pathway for regeneration block.** *Annu Rev Neurosci* 2004, **27**(1:341–368.
8. McKerracher L, David S, Jackson DL, Kottis V, Dunn RJ, Braun PE: **Identification of myelin-associated glycoprotein as a major myelin-derived inhibitor of neurite growth.** *Neuron* 1994, **13**(4):805–811.
9. Wang KC, Koprivica V, Kim JA, *et al*: **Oligodendrocyte-myelin glycoprotein is a Nogo receptor ligand that inhibits neurite outgrowth.** *Nature* 2002, **417**(6892):941–944.
10. Bradbury EJ, Moon LD, Popat RJ, *et al*: **Chondroitinase ABC promotes functional recovery after spinal cord injury.** *Nature* 2002, **416**(6881):636–640.
11. McKeon RJ, Schreiber RC, Rudge JS, Silver J: **Reduction of neurite outgrowth in a model of glial scarring following CNS injury is correlated with the expression of inhibitory molecules on reactive astrocytes.** *J Neurosci* 1991, **11**(11):3398–3411.
12. De Winter F, Holtmaat AJ, Verhaagen J: **Neuropilin and class 3 semaphorins in nervous system regeneration.** *Adv Exp Med Biol* 2002, **515**:115–139.
13. Pasterkamp RJ, Giger RJ, Ruitenberg MJ, *et al*: **Expression of the gene encoding the chemorepellent semaphorin III is induced in the fibroblast component of neural scar tissue formed following injuries of adult but not neonatal CNS.** *Mol Cell Neurosci* 1999, **13**(2):143–166.
14. Hata K, Fujitani M, Yasuda Y, *et al*: **RGMa inhibition promotes axonal growth and recovery after spinal cord injury.** *J Cell Biol* 2006, **173**(1):47–58.
15. Schwab JM, Conrad S, Monnier PP, Julien S, Mueller BK, Schluesener HJ: **Spinal cord injury-induced lesional expression of the repulsive guidance molecule (RGM).** *Eur J Neurosci* 2005, **21**(6):1569–1576.
16. Kim JE, Li S, GrandPre T, Qiu D, Strittmatter SM: **Axon regeneration in young adult mice lacking Nogo-A/B.** *Neuron* 2003, **38**(2):187–199.
17. Simonen M, Pedersen V, Weinmann O, *et al*: **Systemic deletion of the myelin-associated outgrowth inhibitor Nogo-A improves regenerative and plastic responses after spinal cord injury.** *Neuron* 2003, **38**(2):201–211.
18. Taniguchi M, Yuasa S, Fujisawa H, *et al*: **Disruption of semaphorin III/D gene causes severe abnormality in peripheral nerve projection.** *Neuron* 1997, **19**(3):519–530.
19. Kikuchi K, Kishino A, Konishi O, *et al*: **In vitro and in vivo characterization of a novel semaphorin 3A inhibitor, SM-216289 or xanthofulvin.** *J Biol Chem* 2003, **278**(44):42985–42991.
20. Kaneko S, Iwanami A, Nakamura M, *et al*: **A selective Sema3A inhibitor enhances regenerative responses and functional recovery of the injured spinal cord.** *Nat Med* 2006, **12**(12):1380–1389.
21. García-Alías G, Barkhuysen S, Buckle M, Fawcett JW: **Chondroitinase ABC treatment opens a window of opportunity for task-specific rehabilitation.** *Nat Neurosci* 2009, **12**(9):1145–1151.
22. Heng C, de Leon RD: **Treadmill training enhances the recovery of normal stepping patterns in spinal cord contused rats.** *Exp Neurol* 2009, **216**(1):139–147.
23. Winchester P, McColl R, Querry R, *et al*: **Changes in supraspinal activation patterns following robotic locomotor therapy in motor-incomplete spinal cord injury.** *Neurorehabil Neural Repair* 2005, **19**(4):313–324.
24. Courtine G, Gerasimenko Y, van den Brand R, *et al*: **Transformation of nonfunctional spinal circuits into functional states after the loss of brain input.** *Nat Neurosci* 2009, **12**(10):1333–1342.
25. Barbeau H, Rossignol S: **Recovery of locomotion after chronic spinalization in the adult cat.** *Brain Res* 1987, **412**(1):84–95.
26. Kubasak MD, Hedlund E, Roy RR, Carpenter EM, Edgerton VR, Phelps PE: **L1 CAM expression is increased surrounding the lesion site in rats with complete spinal cord transection as neonates.** *Exp Neurol* 2005, **194**(2):363–375.
27. Ichiyama R, Gerasimenko Y, Zhong H, Roy R, Edgerton V: **Hindlimb stepping movements in complete spinal rats induced by epidural spinal cord stimulation.** *Neurosci Lett* 2005, **383**(3):339–344.
28. Kubasak MD, Jindrich DL, Zhong H, *et al*: **OEG implantation and step training enhance hindlimb-stepping ability in adult spinal transected rats.** *Brain* 2007, **131**(1):264–276.
29. Acevedo LM, Barillas S, Weis SM, Gothert JR, Cheresh DA: **Semaphorin 3A suppresses VEGF-mediated angiogenesis yet acts as a vascular permeability factor.** *Blood* 2008, **111**(5):2674–2680.

30. Kolodkin AL, VD L, *et al*: **neuropilin is a semaphorin III receptor.** *Cell* 1997, **90**:753–762.
31. Guizarsahagun G, Ibarra A, Espitia A, Martinez A, Madrazo I, Francobourland R: **Glutathione monoethyl ester improves functional recovery, enhances neuron survival, and stabilizes spinal cord blood flow after spinal cord injury in rats.** *Neuroscience* 2005, **130**(3):639–649.
32. Imperato-Kalmar EL, McKinney RA, Schnell L, Rubin BP, Schwab ME: **Local changes in vascular architecture following partial spinal cord lesion in the rat.** *Exp Neurol* 1997, **145**(2 Pt 1):322–328.
33. Loy DN, Crawford CH, Darnall JB, Burke DA, Onifer SM, Whittemore SR: **Temporal progression of angiogenesis and basal lamina deposition after contusive spinal cord injury in the adult rat.** *J Comp Neurol* 2002, **445**(4):308–324.
34. Casella GTB, Marcillo A, Bunge MB, Wood PM: **New vascular tissue rapidly replaces neural parenchyma and vessels destroyed by a contusion injury to the Rat spinal cord.** *Exp Neurol* 2002, **173**(1):63–76.
35. Kitamura K, Iwanami A, Nakamura M, *et al*: **Hepatocyte growth factor promotes endogenous repair and functional recovery after spinal cord injury.** *J Neurosci Res* 2007, **85**(11):2332–2342.
36. Piaton G, Aigrot MS, Williams A, *et al*: **Class 3 semaphorins influence oligodendrocyte precursor recruitment and remyelination in adult central nervous system.** *Brain* 2011, **134**(4):1156–1167.
37. Kiehn O: **Locomotor circuits in the mammalian spinal cord.** *Annu Rev Neurosci* 2006, **29**:279–306.
38. Kiehn O, Kjaerulff O: **Distribution of central pattern generators for rhythmic motor outputs in the spinal cord of limbed vertebrates.** *Ann N Y Acad Sci* 1998, **860**:110–129.
39. Gulino R, Dimartino M, Casabona A, Lombardo SA, Perciavalle V: **Synaptic plasticity modulates the spontaneous recovery of locomotion after spinal cord hemisection.** *Neurosci Res* 2007, **57**(1):148–156.
40. Ying Z, Roy R, Edgerton V, Gomezpinilla F: **Exercise restores levels of neurotrophins and synaptic plasticity following spinal cord injury.** *Exp Neurol* 2005, **193**(2):411–419.
41. Ahn SN, Guu JJ, Tobin AJ, Edgerton VR, Tillakaratne NJ: **Use of c-fos to identify activity-dependent spinal neurons after stepping in intact adult rats.** *Spinal Cord* 2006, **44**(9):547–559.
42. Huang A, Noga B, Carr P, Fedirchuk B, Jordan L: **Spinal cholinergic neurons activated during locomotion: localization and electrophysiological characterization.** *J Neurophysiol* 2000, **83**:3537–3547.
43. Ichiyama RM, Courtine G, Gerasimenko YP, *et al*: **Step training reinforces specific spinal locomotor circuitry in adult spinal rats.** *J Neurosci* 2008, **28**(29):7370–7375.
44. de Leon RD, Acosta CN: **Effect of robotic-assisted treadmill training and chronic quipazine treatment on hindlimb stepping in spinally transected rats.** *J Neurotrauma* 2006, **23**(7):1147–1163.
45. Maier IC, Ichiyama RM, Courtine G, *et al*: **Differential effects of anti-Nogo-A antibody treatment and treadmill training in rats with incomplete spinal cord injury.** *Brain* 2009, **132**(6):1426–1440.
46. Bareyre FM, Kerschensteiner M, Raineteau O, Mettenleiter TC, Weinmann O, Schwab ME: **The injured spinal cord spontaneously forms a new intraspinal circuit in adult rats.** *Nat Neurosci* 2004, **7**(3):269–277.
47. Raineteau O, Schwab ME: **Plasticity of motor systems after incomplete spinal cord injury.** *Nat Rev Neurosci* 2001, **2**:263–273.
48. Courtine G, Song B, Roy RR, *et al*: **Recovery of supraspinal control of stepping via indirect propriospinal relay connections after spinal cord injury.** *Nat Med* 2008, **14**(1):69–74.
49. Dunlop SA: **Activity-dependent plasticity: implications for recovery after spinal cord injury.** *Trends Neurosci* 2008, **31**(8):410–418.
50. Kiehn O, Kjaerulff O: **Spatiotemporal characteristics of 5-HT and dopamine-induced rhythmic hindlimb activity in the in vitro neonatal rat.** *J Neurophysiol* 1996, **75**(4):1472–1482.
51. Feraboli-Lohnherr D, Orsal D, Yakovleff A, Gimenez y Ribotta M, Privat A: **Recovery of locomotor activity in the adult chronic spinal rat after sublesional transplantation of embryonic nervous cells: specific role of serotonergic neurons.** *Exp Brain Res* 1997, **113**(3):443–454.
52. Edgerton VR, Tillakaratne NJK, Bigbee AJ, de Leon RD, Roy RR: **Plasticity of the spinal neural circuitry after injury.** *Annu Rev Neurosci* 2004, **27**(1):145–167.
53. Cote MP, Menard A, Gossard JP: **Spinal cats on the treadmill: changes in load pathways.** *J Neurosci* 2003, **23**(7):2789–2796.
54. Nave K-A: **Myelination and support of axonal integrity by glia.** *Nature* 2010, **468**(7321):244–252.
55. Nessler JA, Timoszyk W, Merlo M, *et al*: **A robotic device for studying rodent locomotion after spinal cord injury.** *IEEE Trans Neural Syst Rehabil Eng* 2005, **13**(4):497–506.
56. Timoszyk W, Nessler J, Acosta C, *et al*: **Hindlimb loading determines stepping quantity and quality following spinal cord transection.** *Brain Res* 2005, **1050**(1–2):180–189.
57. Molander C, Xu Q, Grant G: **The cytoarchitectonic organization of the spinal cord in the rat. I. The lower thoracic and lumbosacral cord.** *J Comp Neurol* 1984, **230**(1):133–141.
58. Wang D, Ichiyama RM, Zhao R, Andrews MR, Fawcett JW: **Chondroitinase combined with rehabilitation promotes recovery of forelimb function in rats with chronic spinal cord injury.** *J Neurosci* 2011, **31**(25):9332–9344.
59. Zheng B, Ho C, Li S, Keirstead H, Steward O, Tessier-Lavigne M: **Lack of enhanced spinal regeneration in Nogo-deficient mice.** *Neuron* 2003, **38**(2):213–224.

doi:10.1186/1756-6606-7-14
Cite this article as: Zhang *et al.*: Rewiring of regenerated axons by combining treadmill training with semaphorin3A inhibition. *Molecular Brain* 2014 **7**:14.

PLOS | ONE

RESEARCH ARTICLE

Polarity Specific Effects of Transcranial Direct Current Stimulation on Interhemispheric Inhibition

Toshiki Tazoe[1,2*¤], Takashi Endoh[1,3], Taku Kitamura[1,4], Toru Ogata[1]

1. Department of Rehabilitation for Movement Functions, Research Institute, National Rehabilitation Center for Persons with Disabilities, Tokorozawa, Japan, **2.** Japan Society for the Promotion of Science, Tokyo, Japan, **3.** Faculty of Child Development and Education, Uekusa Gakuen University, Chiba, Japan, **4.** Division of Functional Control Systems, Graduate School of Engineering and Science, Shibaura Institute of Technology, Saitama, Japan

*Tot12@pitt.edu

¤ Current address: Systems Neuroscience Institute, Center for the Neural Basis of Cognition, University of Pittsburgh, 4074 BST4, 3501 Fifth Avenue, Pittsburgh, PA, United States of America.

OPEN ACCESS

Citation: Tazoe T, Endoh T, Kitamura T, Ogata T (2014) Polarity Specific Effects of Transcranial Direct Current Stimulation on Interhemispheric Inhibition. PLoS ONE 9(12): e114244. doi:10.1371/journal.pone.0114244

Editor: Nicholas P. Holmes, University of Reading, United Kingdom

Received: July 24, 2014

Accepted: November 5, 2014

Published: December 5, 2014

Data Availability: The authors confirm that all data underlying the findings are fully available without restriction. All relevant data are within the paper.

Funding: This research was supported by Grants-in-Aid for Research Fellow of the Japan Society for the Promotion of Science to TT (#23·10759) and by Grants-in-Aids for Young Scientist B to TE (#24700612). The funders had no role in study design, data collection and analysis, decision to publish, or preparation of the manuscript.

Competing Interests: The authors have declared that no competing interests exist.

Abstract

Transcranial direct current stimulation (tDCS) has been used as a useful interventional brain stimulation technique to improve unilateral upper-limb motor function in healthy humans, as well as in stroke patients. Although tDCS applications are supposed to modify the interhemispheric balance between the motor cortices, the tDCS after-effects on interhemispheric interactions are still poorly understood. To address this issue, we investigated the tDCS after-effects on interhemispheric inhibition (IHI) between the primary motor cortices (M1) in healthy humans. Three types of tDCS electrode montage were tested on separate days; anodal tDCS over the right M1, cathodal tDCS over the left M1, bilateral tDCS with anode over the right M1 and cathode over the left M1. Single-pulse and paired-pulse transcranial magnetic stimulations were given to the left M1 and right M1 before and after tDCS to assess the bilateral corticospinal excitabilities and mutual direction of IHI. Regardless of the electrode montages, corticospinal excitability was increased on the same side of anodal stimulation and decreased on the same side of cathodal stimulation. However, neither unilateral tDCS changed the corticospinal excitability at the unstimulated side. Unilateral anodal tDCS increased IHI from the facilitated side M1 to the unchanged side M1, but it did not change IHI in the other direction. Unilateral cathodal tDCS suppressed IHI both from the inhibited side M1 to the unchanged side M1 and from the unchanged side M1 to the inhibited side M1. Bilateral tDCS increased IHI from the facilitated side M1 to the inhibited side M1 and attenuated IHI in the opposite direction. Sham-tDCS affected neither corticospinal excitability nor IHI. These findings indicate that tDCS produced

polarity-specific after-effects on the interhemispheric interactions between M1 and that those after-effects on interhemispheric interactions were mainly dependent on whether tDCS resulted in the facilitation or inhibition of the M1 sending interhemispheric volleys.

Introduction

Transcranial direct current stimulation (tDCS) is a widely used interventional brain stimulation technique that improves unilateral upper-limb motor function in healthy humans [1–6] and hemiparetic stroke patients [7–11]. Based on the polarity-specific after-effects [12], anodal tDCS is applied to the motor cortex innervating the target limb muscles to enhance corticospinal excitability [5, 8], and cathodal tDCS targets the contralateral motor cortex to suppress the contralateral corticospinal excitability [5, 9], which is assumed to contribute to the reduction of transcallosal inhibition from the contralateral side of the primary motor cortex (M1) to the target M1 side [13, 14]. Based on these strategies, recently, anodal and cathodal tDCS are simultaneously applied to one motor cortex and the other, respectively (bilateral tDCS) [3, 5, 6, 10, 15–20]. Bilateral tDCS is supposed to combine the effects of anodal and cathodal tDCS and result in larger after-effects compared with unilateral tDCS [3, 10]. However, the advantage of bilateral tDCS is still under debate [15–17, 19] because it has not been fully elucidated how tDCS affects transcallosal inhibition underlying interhemispheric balance between motor cortices.

Studies using transcranial magnetic stimulation (TMS) have demonstrated that transcallosal inhibition is affected by the modulation of intracortical motor circuits in both M1 that project and receive callosal volleys [21–24]. Hence, it is possible that tDCS-induced neuromodulation in the M1 neural circuits affects transcallosal inhibition. Indeed, Lang et al. [25] demonstrated that transcallosal inhibition measured by the duration of ipsilateral silent period (iSP) was increased and decreased by anodal and cathodal tDCS, respectively, that were unilaterally delivered to the motor cortex receiving transcallosal inhibition. However, the robust effects on iSP were not observed after unilateral tDCS given to the motor cortex projecting callosal volleys [25]. These findings may not be in line with the idea that tDCS given to a motor cortex influences the contralateral motor cortex through the modulation of transcallosal pathways. Subsequently, Williams et al. [5] investigated short-interval interhemispheric inhibition (IHI) elicited by paired-pulse TMS and found that IHI was suppressed after the application of bilateral tDCS combined with unimanual motor training. Although the reduction of IHI was accompanied by the decrease of corticospinal excitability in the side of motor cortex projecting callosal volleys, their causal association was not fully elucidated [5].

IHI and iSP are thought to be mediated by different neuronal populations in the transcallosal pathways [26], suggesting the possibility that tDCS does not affect their different neuronal populations in a similar way. Indeed, Gilio et al. [27] demonstrated that 1 Hz repetitive TMS (rTMS) given to the left M1 suppressed IHI from the left M1 to right M1 with minor effects on iSP. Given these physiological backgrounds, we hypothesized that tDCS given at rest would induce polarity-specific after-effects on IHI from the stimulated M1 in which the corticospinal excitability was changed. To examine this hypothesis, we investigated the after-effects of tDCS applied at rest with three different electrode montages (i.e., unilateral anodal, unilateral cathodal, and bilateral). Each montage was intended to elicit either facilitation of right corticospinal excitability, inhibition of left corticospinal excitability, or both. It should be noted that the intended relative change between the left and right corticospinal excitabilities was the same across the three electrode montages, with right greater than left. Before and after each tDCS, single-pulse TMS and paired-pulse TMS were given to the left M1 and right M1 in order to assess the corticospinal excitability and mutual direction of IHI.

Methods

Participants

Participants were sixteen healthy right-handed volunteers (22–34 years old, 3 females). All participants gave their written informed consent to participate in this study. The experimental and consent procedures were approved by the ethical review board of the National Rehabilitation Center for Persons with Disabilities and which was in accordance with the guidelines established in the Declaration of Helsinki. All participants were naïve to the purpose of the experiments.

Recordings

Electromyography (EMG) was recorded from the bilateral first dorsal interosseous (FDI) muscles. Self-adhesive Ag/AgCl electrodes were placed over the muscle belly and the metacarpophalangeal joint. The EMG signals were amplified and filtered (bandwidth, 20–3000 Hz) with a conventional bioamplifier (BIOTOP 6R12, NEC San-ei, Tokyo, Japan). Their digital data were acquired with a sampling rate of 5 kHz with a CED 1401 A/D converter (Cambridge Electronic Design, Cambridge, UK) and stored on a computer for off-line analysis.

TMS

Corticospinal excitability and IHI were investigated by single-pulse and paired-pulse TMS, respectively. TMS was delivered to the left M1 and the right M1 with a figure 8-shaped coil (70-mm diameter) connected to a Magstim 200 (Magstim, Whitland, UK). The stimulus location was determined to be the hot spot where weak stimulation could elicit the largest motor evoked potential (MEP) in the FDI

muscle. The coil was held tangentially over the scalp with the handle pointing backward and 45° lateral away from the midline. The resting motor threshold (RMT) was defined as the minimum stimulus intensity that produced MEPs that were greater than 50 μV in at least 5 out of 10 consecutive trials. For the single-pulse TMS, the intensity of test stimulation (TS) was set at 120% of the RMT. Stimuli were consecutively delivered about every 10 s. Both the left and right hemispheres were examined sequentially with a randomized order across the participants. Fifteen MEPs were obtained at each hemisphere. Paired-pulse TMS was used to elicit IHI both from the left M1 to the right M1 and from the right M1 to the left M1. A suprathreshold conditioning stimulation (CS) with an intensity at 120% of RMT was delivered to M1 on one side 10 ms before a TS was delivered to M1 on the other side. For a few participants, it was impossible to place both coils at the optimal direction due to the size of the coil. Thus, the handle of the coil for the CS was pointed backward and more than 45° away from the midline until both coils did not contact each other. The TS intensity was adjusted so that the peak-to-peak amplitude of the MEP was about 1 mV. The paired-pulse stimulation and TS alone were randomly given every 10 s. Fifteen control MEPs and 15 conditioned MEPs were obtained at each side of tested FDI. For both single-pulse and paired-pulse TMS, if trials showed more than 20 μV of EMG activity in the window of 100 ms before TMS, additional stimuli were given instead of those trials.

tDCS

Direct current stimulation was delivered by a battery-driven constant-current stimulator (Eldith DC-Stimulator, NeuroConn, Ilmenau, Germany) through a pair of rubber electrodes (5 × 5 cm) covered with saline-soaked sponges (5 × 6 cm). We examined three kinds of electrode montages; anodal tDCS over the right M1, cathodal tDCS over the left M1, and bilateral tDCS over the right M1 and left M1. For anodal tDCS, the anode and cathode were positioned on the right M1 (i.e., the hot spot of the left FDI) and the superior edge of the left orbit, respectively (Figure 1A). For cathodal tDCS the anode and cathode were positioned on the superior edge of the right orbit and the left M1 (i.e., the hot spot of the right FDI), respectively (Figure 1B). For bilateral tDCS, the anode and cathode were over the right M1 and left M1, respectively (Figure 1C). The current polarity at each electrode was masked to the participants. 1.5 mA of direct current stimulation was delivered for 15 min. The current was gradually increased and decreased during the first and last 10 s of the stimulation, respectively. Sham-tDCS was conducted for 15 min with the montages of anodal tDCS and bilateral tDCS (Figure 1D, E). The 1.5 mA of direct current stimulation was delivered for first 30 s subsequent to 10 s of current increment.

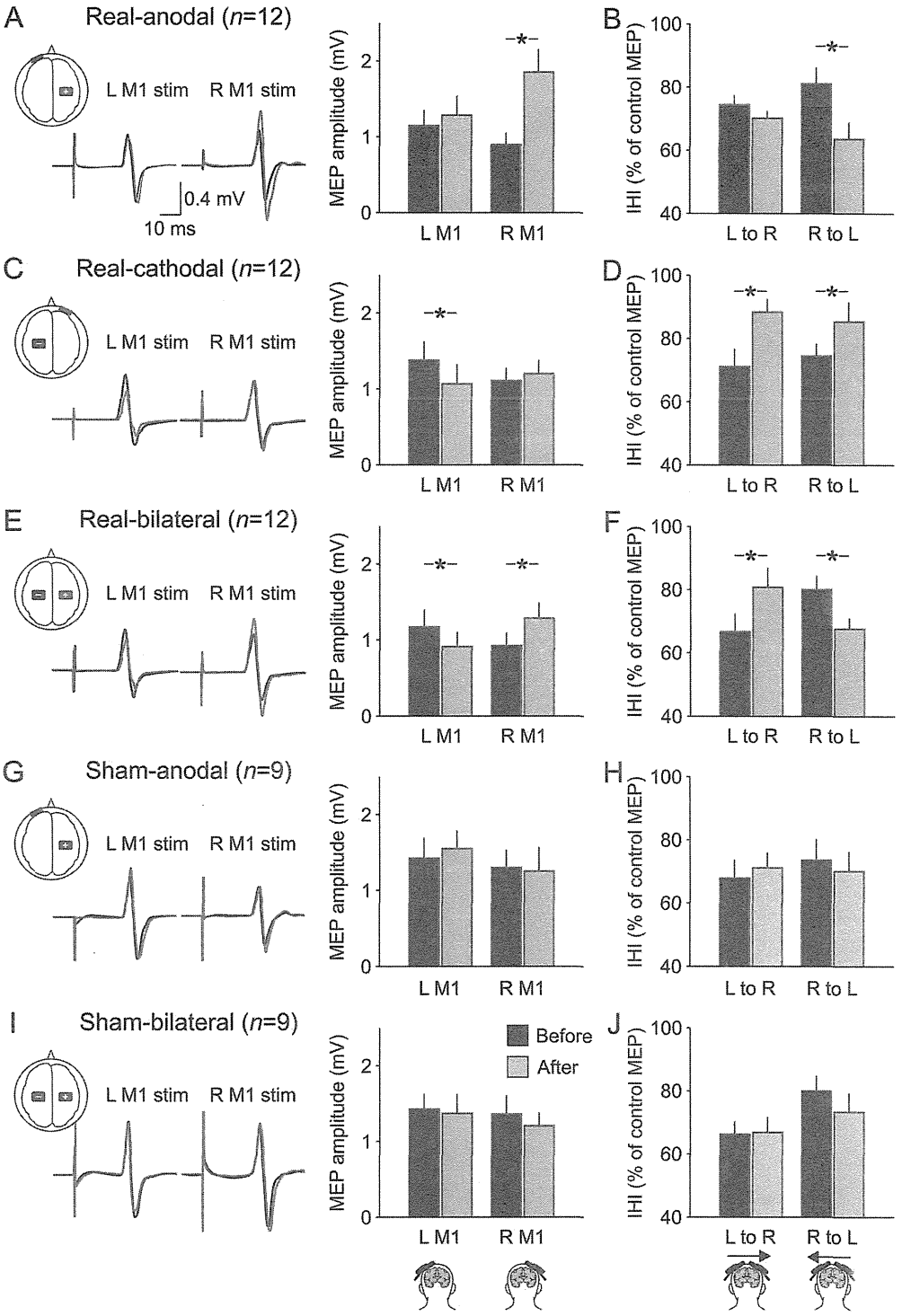

Figure 1. tDCS after-effects on MEPs and IHI. From top to bottom, real-anodal tDCS (A, B), real-cathodal tDCS (C, D), real-bilateral tDCS (E, F), sham-anodal tDCS (G, H), and sham-bilateral tDCS (I, J). The left and right sides of the traces are MEPs that are elicited by single-pulse TMS over the left M1 and right M1, respectively. The black and gray lines indicate MEPs that were elicited before and after DCS, respectively. The left bar graphs (A, C, E, G, J) show the average data of MEP of all participants. The sets of the left- and the right-sided columns represent MEP amplitude elicited by left (L) M1 stimulation and right (R) M1 stimulation, respectively. The rights bar graphs (B, D, F, H, J) show the average data of IHI of all participants.

IHI was expressed as the ratio of the conditioned MEP amplitude normalized by the control MEP amplitude (i.e., larger value indicates less IHI). The sets of the left- and right-sided columns represent IHI from the left M1 to the right one (L to R) and that from the right M1 to the left one (R to L), respectively. The black and gray columns represent before and after tDCS, respectively. Error bas show standard error of means. The asterisks indicate a significant difference; * $p<0.05$.

doi:10.1371/journal.pone.0114244.g001

Experimental procedures

The experiments were composed of real-tDCS and sham-tDCS sessions. 12 participants joined the real-tDCS session and 9 participants joined the sham-tDCS session. 5 out of 16 participants were involved in both sessions; three of them participated in the real-tDCS session first and two of them participated in the sham-tDCS session first. Each kind of electrode montage was tested on a different day. At least 3 weeks were interleaved across the experimental days. At each tDCS session, the order of the electrode montages was randomized across participants. In the experiments, the participants sat comfortably on a reclining chair with their shoulders and elbows semi-flexed. Both of their hands were placed on the table with palms downward. Before the tDCS application, RMT was measured in both M1. Then, the single-pulse and paired-pulse TMS protocols were conducted. After these baseline measurements were made, real- or sham-tDCS with an electrode montage was given for 15 min. After tDCS application, the same measurements were conducted on each side of M1.

Data analysis

For the evaluation of corticospinal excitability, the peak-to-peak amplitudes of the MEPs elicited by single-pulse TMS were measured in the window 18–50 after the TMS trigger. The extent of after-effects was expressed as the ratio of the MEP amplitude obtained after tDCS to the baseline MEP amplitude obtained before tDCS. In order to evaluate IHI, the amplitude of the conditioned MEPs elicited by paired-pulse stimulation were normalized by the amplitude of the control MEPs evoked by TS alone. Trials with more than 20 μV of peak-to-peak amplitude in background EMG activity for 100 ms pre-stimulus period were discarded from the analysis. For the statistical analysis, a three-way analysis of variance (ANOVA) with repeated measures was performed with factors of time (before and after tDCS), tDCS type (real-anodal, real-cathodal, real-bilateral, sham-anodal, sham-bilateral), and TS side (left and right M1). In case a significant interaction between three factors was obtained, appropriate follow-up two-way ANOVA was conducted to examine the interaction of time and TS side factors at each tDCS type. In order to compare the magnitude of after-effects across conditions, one-way ANOVA with repeated measures was conducted with factor of tDCS type at each TS side. For the comparison of baseline level in each measurement, two-way ANOVA with repeated measures was performed with factors of tDCS type and TS side. *Post-hoc* comparisons were conducted by Tukey's test.

According to the findings in the previous studies [12, 16], we expected that real-tDCS induced the polarity-specific modulation in the M1 underneath the active electrode. Thus, we anticipated that real-tDCS influenced the excitability of callosal neurons in the same M1. Therefore, to examine the relationship between the after-effects on MEP amplitude and IHI, we also conducted Pearson correlation analysis in the real-tDCS after-effects between MEP amplitude and IHI. *P* values less than 0.05 were recognized as statistically significant in all analyses. Group data are presented as the mean ± standard deviation in the text.

Results

RMT, MEP

RMT was different across TS sides ($F_{1,49}=5.53$, $p=0.02$). TMS given to the left M1 showed slightly lower RMT than the right M1 (Table 1). However, tDCS did not affect RMT ($F_{1,49}=0.43$, $p=0.51$) regardless of tDCS type ($F_{4,49}=0.70$, $p=0.59$). Three-way ANOVA did not show any significant interactions (time × tDCS type, $F_{4,49}=0.07$, $p=0.99$; time × TS side, $F_{1,49}=0.26$, $p=0.62$; tDCS type × TS side, $F_{4,49}=0.24$, $p=0.92$; time × tDCS type × TS side, $F_{4,49}=1.00$, $p=0.42$).

Figure 1A illustrates representative example of MEPs elicited before and after tDCS. Consistent with the findings in the previous studies [12, 16], facilitation and inhibition were observed in the MEPs elicited by single-pulse TMS over the M1 under the anode and the cathode, respectively. Three-way ANOVA revealed significant interactions of time and tDCS type and TS side ($F_{4,49}=4.39$, $p=0.004$) on MEP amplitude, indicating that the interaction of time and TS side was dependent on the tDCS type. Then, we performed follow-up two-way ANOVA for each tDCS type. Regardless of electrode montage, real-tDCS showed significant interaction of time and TS side (real-anodal, $F_{1,11}=8.32$, $p=0.02$; real-cathodal, $F_{1,11}=5.76$, $p=0.04$; real-bilateral, $F_{1,11}=23.53$, $p<0.001$), indicating that all electrode montage had tDCS after-effect on MEP amplitude such that their tDCS after-effects were different depending on the TS side. *Post-hoc* analysis revealed that after real-anodal tDCS over the right M1, the MEP elicited from the right M1 was increased (232.0 ± 144.7%, $p<0.001$) and the MEP elicited from the left M1 was unchanged (111.1 ± 41.7%, $p=0.54$) compared with the baseline (Figure 1A). After real-cathodal tDCS over the left M1, the MEP elicited from the left M1 was decreased (76.2 ± 27.6%, $p=0.01$) and the MEP elicited from the right M1 was unchanged (109.0 ± 36.5%, $p=0.45$, Figure 1C). After real-bilateral tDCS (anode over the right M1, cathode over the left M1), the MEP elicited from the right M1 was increased (157.6 ± 68.2%, $p<0.001$) and the MEP elicited from the left M1 was decreased (75.4 ± 28.3%, $p=0.01$, Figure 1E). In contrast to real-tDCS, nether of sham-tDCS showed significant main effect of time (sham-anodal, $F_{1,8}=0.38$, $p=0.55$; sham-bilateral, $F_{1,8}=1.36$, $p=0.28$) or TS side (sham-anodal, $F_{1,8}=1.17$, $p=0.31$; sham-bilateral, $F_{1,8}=0.66$, $p=0.44$), or their interaction (sham-anodal, $F_{1,8}=2.68$, $p=0.14$; sham-bilateral, $F_{1,8}=0.05$, $p=0.84$, Figure 1G, I). Two-way ANOVA revealed that baseline level of MEP amplitude before tDCS was not

Table 1. Resting motor threshold (% maximal stimulator output).

		Real-tDCS (n=12)			Sham-tDCS (n=9)	
		Anodal	Cathodal	Bilateral	Anodal	Bilateral
Left M1	Before	43.8±6.1	44.7±6.9	43.8±6.8	46.1±7.6	46.6±7.5
	After	43.5±5.5	45.0±7.8	44.4±6.5	46.0±7.6	46.0±7.6
Right M1	Before	44.7±6.0	46.8±9.8	45.7±8.1	48.3±7.6	48.4±5.6
	After	44.2±6.5	46.1±10.7	44.7±8.9	48.6±7.0	48.9±6.7

Values are mean ± standard deviation.

doi:10.1371/journal.pone.0114244.t001

different across tDCS types ($F_{4,49}$=0.96, p=0.44) or TS sides ($F_{1,49}$=3.79, p=0.06) with no interaction of their factors ($F_{4,49}$=0.07, p=0.99).

To sum up, facilitation and inhibition were observed in the MEPs elicited from the M1 under the anode and the cathode, respectively. With real-anodal and real-cathodal tDCS, the MEP elicited from the unstimulated M1 was unchanged. The magnitude of after-effects was not different across the conditions that showed significant facilitation (real-anodal 232.0±144.7%, real-bilateral 157.6±68.2%, p=0.20) or inhibition (real-cathodal 76.2±27.6%, real-bilateral 75.4±28.3%, p=0.99).

IHI

Both before and after tDCS, IHI was examined both from the left M1 to the right M1 and from the right M1 to the left M1. By adjusting the TS intensity to elicit a 1 mV MEP, the amplitude of the control MEP was not different across conditions. Three-way ANOVA revealed significance of neither main effect of time ($F_{1,49}$=0.07, p=0.80), tDCS type ($F_{4,49}$=0.1.74, p=0.16), TS side ($F_{1,49}$=0.33, p=0.57), nor their interactions (time × tDCS type, $F_{4,49}$=0.76, p=0.59; time × TS side, $F_{1,49}$=0.10, p=0.76; tDCS type × TS side, $F_{4,49}$=0.40, p=0.81; time × tDCS type × TS side, $F_{4,49}$=0.24, p=0.91).

The three-way repeated measures ANOVA revealed significant interaction of time and tDCS type and TS side ($F_{4,49}$=2.64, p=0.04) on IHI, indicating that the interaction of time and TS side was dependent on the tDCS type. Then, we performed follow-up two-way ANOVA for each tDCS type. Real-anodal and real-bilateral tDCS showed significant interaction of time and TS side (real-anodal, $F_{1,11}$=8.36, p=0.02; real-bilateral, $F_{1,11}$=20.08, p<0.001). On the other hand, real-cathodal tDCS had only main effect of time ($F_{1,8}$=9.42, p=0.01) but not main effect of TS side ($F_{1,8}$=0.001, p=0.98) or interaction of time and TS side ($F_{1,8}$=1.78, p=0.21). That is, in the real-tDCS session, all electrode montages had tDCS after-effect on IHI. The tDCS after-effect was different depending on the TS side (i.e., direction of IHI) after real-anodal and real-bilateral tDCS. On the other hand, the after-effect of real-cathodal tDCS was independent of TS side. *Post-hoc* analysis demonstrated that after real-anodal tDCS over the right M1, IHI from the right M1 to the left M1 was significantly increased compared with baseline

($p<0.001$). However, IHI from the left M1 to the right M1 was unchanged ($p=0.16$, Figure 1B). After real-cathodal tDCS over the left M1, a reduction in IHI magnitude was observed both from the left M1 to the right M1 and from the right M1 to the left M1 ($p=0.01$, Figure 1D). After real-bilateral tDCS (anode over the right M1, cathode over the left M1), IHI from the left M1 to the right M1 was decreased compared with baseline ($p=0.001$). In contrast, IHI from the right M1 to the left M1 was increased compared with baseline ($p=0.003$; Figure 1F). Again, neither of sham-tDCS affected IHI (Figure 1H, J). Two-way repeated measures ANOVA did not show any significant effect of time (sham-anodal, $F_{1,8}=0.0003$, $p=0.99$; sham-bilateral, $F_{1,8}=0.28$, $p=0.61$), TS side (sham-anodal, $F_{1,8}=0.11$, $p=0.75$; sham-bilateral, $F_{1,8}=5.10$, $p=0.06$), or their interaction (sham-anodal, $F_{1,8}=0.62$, $p=0.45$; sham-bilateral, $F_{1,8}=1.68$, $p=0.23$). Baseline level of IHI before tDCS was generally larger from the left M1 to the right M1 than the opposite direction. Two-way repeated measures ANOVA showed significant effect of TS side on the baseline level of IHI ($F_{1,49}=10.78$, $p=0.002$), but not main effect of tDCS type ($F_{4,49}=0.40$, $p=0.81$) or interaction of tDCS type and TS side ($F_{4,49}=0.67$, $p=0.62$), indicating that although an asymmetry of IHI was observed across IHI directions, the baselines of IHI on each direction was similar level across tDCS types.

In summary, IHI from the M1 under the anode was increased. In contrast, IHI from the M1 under the cathode was decreased. IHI from the unstimulated M1 showed a decrease after cathodal tDCS, but it was unchanged after anodal tDCS. Finally, we tested the correlation of tDCS after-effects between MEP amplitude and IHI. However, we did not find any significant correlations between the modulations of MEP amplitude and IHI regardless of TS side (Table 2).

Discussion

The present study demonstrated that tDCS produced polarity-specific after-effects on IHI from the stimulated M1 at which the corticospinal excitability was changed. Regardless of unilateral or bilateral tDCS, IHI was generally increased from the M1 at which the corticospinal excitability was increased and decreased from the M1 at which the corticospinal excitability was decreased. Bilateral tDCS simultaneously produced the opposite directional modulation in IHI from the left to the right M1 and in IHI from the right to the left M1 in addition to the bidirectional corticospinal modulation. Although unilateral anodal tDCS did not affect the corticospinal excitability at the side of unstimulated hemisphere or IHI from the M1 on that unstimulated hemisphere, unilateral cathodal tDCS suppressed IHI from the M1 on the unstimulated hemisphere even though the corticospinal excitability was unchanged at the unstimulated side.

In most cases, the modulations of IHI were parallel to the modulations of corticospinal excitability at the side sending callosal volleys. Thus, it is likely that the tDCS after-effects on IHI are relevant with the excitability change in the motor cortex sending callosal volleys. However, we did not observe any significant

Table 2. Relationships in the after-effects of real-tDCS on MEP amplitude and IHI.

Measurements		Electrode montage					
		Anodal		Cathodal		Bilateral	
MEP	IHI	*r* value	*p* value	*r* value	*p* value	*r* value	*p* value
Left M1	Left to Right M1	−0.21	0.52	0.35	0.27	0.16	0.62
Left M1	Right to Left M1	−0.01	0.98	−0.30	0.35	−0.28	0.39
Right M1	Left to Right M1	−0.36	0.25	0.05	0.89	−0.27	0.39
Right M1	Right to Left M1	0.21	0.52	0.03	0.92	−0.32	0.31

Values were obtained by Pearson correlation analysis.

doi:10.1371/journal.pone.0114244.t002

relationships between the modulations of MEP amplitude and IHI. If IHI is mainly derived from the collateral discharges of corticospinal neurons and the tDCS-induced modulation in IHI resulted from the changes in collateral discharges, the modulations in MEP amplitude and IHI could have been correlated. Therefore, the modulation of transcallosal pathways could be partly independent of the changes in corticospinal descending pathways. Transcallosal inhibition is assumed to be derived from the discharge of callosal neurons that are distinct from corticospinal neurons [24, 28, 29]. Accordingly, tDCS might have similarly influenced both corticospinal and callosal neurons in the same M1. In some previous studies, IHI has been evaluated by matching the size of CS-induced MEPs in order to normalize the CS effect [24, 30, 31]. However, the adjusted CS intensity may not be sensitive enough to detect the excitability change in callosal neurons when both corticospinal and callosal neurons are modulated in parallel [24, 31, 32]. In the present study, we used the same CS intensity across before and after the tDCS sessions according to the RMT. Therefore, the modulation of IHI could be observed by detecting parallel modulation in the excitabilities of corticospinal and callosal neurons.

Our findings of the modulation of transcallosal inhibition are partly inconsistent with a previous study that used iSP [25], although the corticospinal excitability was modulated in a similar way. The previous study did not observe changes in iSP from the modulated M1 underneath the tDCS electrode [25]. One possible explanation for this discrepancy may be the differences in the tDCS parameters. The present experiments used a higher intensity (1.5 mA) and a longer duration (15 min) of tDCS compared to the previous study (1.0 mA intensity, 10 min duration). The tDCS after-effects have been shown to increase up to a certain extent of intensity and duration [12, 33, 34]. Furthermore, because the threshold for eliciting transcallosal inhibition is known to be higher than the RMT for MEPs [29, 35–37], callosal neurons might require a relatively high intensity and long duration of tDCS to be modulated. Another possibility is the different neural populations mediating transcallosal inhibition because partly different sets of callosal neurons and target neurons receiving callosal volleys have been assumed to mediate short-interval IHI and iSP [26]. In addition, iSP appears as the inhibition of static voluntary activity, although IHI is the inhibition of

synchronized corticospinal discharges that TMS artificially evokes [29]. Accordingly, such physiological differences might relate to the different susceptibilities to tDCS. Indeed, previous study using rTMS demonstrated the modulation of IHI without robust changes of iSP [27].

We also observed a reduction of IHI from the unchanged M1 after unilateral cathodal tDCS, although unilateral anodal tDCS did not modulate IHI from the unchanged M1. These findings suggested that unilateral tDCS affected interneuronal circuits that presynaptically regulate callosal transmission and/or relay them to the corticospinal neurons [25]. Indeed, tDCS-induced plastic modulation has been shown in some intracortical interneurons that mediate gamma-aminobutyric acid activity [38–40]. One potential reason that unilateral anodal tDCS failed to modulate IHI in this direction might be due to the asymmetry in transcallosal inhibition. Generally, transcallosal inhibition is greater from the left M1 to the right M1 than from the right M1 to the left M1 in right-handers [41, 42], which was also confirmed in our study. Furthermore, previous study reported asymmetric effects of tDCS [4]; tDCS applied over the left dominant hemisphere was more effective than that over the right non-dominant hemisphere. In our study, anodal and cathodal stimuli were given to the different hemispheres. Hence, the lack of modulation of IHI toward the facilitated right-side M1 might be also attributed to the decreased efficiency of tDCS that is applied over the non-dominant hemisphere.

The effect of interventional brain stimulation on transcallosal inhibition has been tested by several stimulation protocols such as low-frequency rTMS [27, 43], theta burst stimulation [44, 45], paired associative stimulation [46], tDCS [5, 25], and quadripulse TMS [47]. Even though their protocols were able to elicit bidirectional modulation on the corticospinal excitability, the modulation of transcallosal inhibition was not always observed [44, 45]. Presumably, the neural elements involving with transcallosal inhibition might have different susceptibilities according to the type of brain stimulation protocol. Although our results show that bilateral tDCS was able to elicit the bidirectional modulation in transcallosal inhibition between left M1 and right M1 in addition to the left and right corticospinal excitabilities, it is worth noting that the extent of MEP modulation by bilateral tDCS was not different compared to that by unilateral tDCS. This finding was also reported in recent studies [16, 17]. Additionally, in line with previous studies [16, 25, 48], neither the polarity of unilateral tDCS affected the corticospinal excitability in the contralateral unstimulated motor cortex even though transcallosal inhibition toward that motor cortex showed short-lasting after-effects (Figure 1). These findings suggest that transcallosal inhibition modulated by tDCS might have minor static effects on the corticospinal excitability in the contralateral motor cortex. Nevertheless, previous studies demonstrated that bilateral tDCS was more effective for improving hand motor performance compared to unilateral anodal tDCS over the target motor cortex [3, 10], and that unilateral cathodal tDCS over a motor cortex results in substantial improvement of ipsilateral hand motor function in healthy [2, 4] and stroke individuals [7, 9, 11, 49]. These facts could provide us rationale to suppose

that suppressed transcallosal inhibition contributes to the contralateral cortical motor activity. Indeed, Williams et al. [5] demonstrated a functional relationship between the suppression of transcallosal inhibition and improvements in motor performance using bilateral tDCS. Conceivably, it might be that a functional role of the decreased transcallosal inhibition can be observed in a time-specific motor event like movement initiation. Transcallosal inhibition is gradually decreased according to the time course of movement initiation [50, 51]. Therefore, a sustained reduction of transcallosal inhibition could contribute to such a situation of motor performance rather than a static enhancement of corticospinal excitability. To support this notion, recent studies using functional magnetic resonance imaging demonstrated that motor task-related M1 activation was greater in bilateral tDCS compared to unilateral anodal tDCS, and that the M1 activation changes in laterality were correlated with microstructural status of transcallosal motor fibers [18] although resting-state interhemispheric functional connectivity between the left M1 and the right M1 did not show after-effects regardless of unilateral anodal or bilateral tDCS [20]. Therefore, it seems conceivable that modulated transcallosal pathways contribute to the motor performances without marked changes in the corticospinal excitability at rest.

From the methodological point of view, we need to consider tDCS parameters as limitations of our study. First, strong intensity and long duration of direct current stimulation has a risk of over stimulating that causes reversing facilitatory effect of cathodal tDCS on the corticospinal excitability. A recent study demonstrated that cathodal tDCS with 2 mA of intensity and 20 min of duration facilitated the corticospinal excitability [52]. Because tDCS with a high intensity (2 mA) and a short duration (5 min) retained the general polarity-specific after-effects [16], the combination of intensity and duration might be a specific factor for the tDCS after-effects. Second, small number of participants should be considered as another limitation. Though we found significant tDCS after-effects on MEP amplitude and IHI, some insignificant results may be due to small sample size. We should make a point that the participants were not completely identical across real-tDCS and sham-tDCS sessions. Finally, our study cannot completely rule out spinal effects [53, 54]. Though IHI was demonstrated to be mediated by cortical circuits through transcallosal pathways [55, 56], potential contribution of subcortical circuits to IHI need to be considered [57].

As a therapeutic tool, tDCS has been frequently applied in patients with hemiparetic stroke [58]. Thus, our findings that tDCS modulated transcallosal inhibition with polarity-specific manner could provide a useful perspective on the understanding of the tDCS therapeutic effect on the recovery of motor function after stroke. In terms of interhemispheric neural modulations, the application of cathodal tDCS to contralesional hemisphere appears to be reliable as demonstrated by some clinical studies [7, 8, 10, 11, 49]. However, we may also need to take into account the tDCS effect on the uncrossed ipsilateral motor pathway [59, 60]. A recent study demonstrated that cathodal tDCS over a motor cortex affected presumed uncrossed cortico-propriospinal pathway [60]. As the severely impaired motor function is potentially compensated by ipsilateral cortical activity

[61], it is important to note the potential risk that cathodal stimulation over ipsilesional hemisphere deteriorates motor function [62].

In conclusion, the present study demonstrated that tDCS produced polarity-specific after-effects on transcallosal inhibition between motor cortices. Comprehensively, IHI was increased from the M1 at which the corticospinal excitability was increased and decreased from the M1 at which the corticospinal excitability was decreased, suggest that tDCS is capable of modulating neuronal activities that are involved with sending and receiving callosal discharges.

Acknowledgments

We would like to thank Dr. Y. Nakajima for his support. We also thank Mr. T. Hoshiba for assistance of data collection.

Author Contributions

Conceived and designed the experiments: TT TE TO. Performed the experiments: TT TE TK. Analyzed the data: TT. Contributed reagents/materials/analysis tools: TT TE TO. Wrote the paper: TT TO.

References

1. **Boggio PS, Castro LO, Savagim EA, Braite R, Cruz VC, et al.** (2006) Enhancement of non-dominant hand motor function by anodal transcranial direct current stimulation. Neurosci Lett 404: 232–236.
2. **Vines BW, Nair DG, Schlaug G** (2006) Contralateral and ipsilateral motor affects after transcranial direct current stimulation. NeuroReport 17: 671–674.
3. **Vines BW, Cerruti C, Schlaug G** (2008) Dual-hemisphere tDCS facilitates greater improvements for healthy subjects' non-dominant hand compared to uni-hemisphere stimulation. BMC Neurosci 9: 103. doi: 10.1186/1471-2202-9-103
4. **Vines BW, Nair D, Schlaug G** (2008) Modulating activity in the motor cortex affects performance for the two hands differently depending upon which hemisphere is stimulated. Eur J Neurosci 28: 1667–1673.
5. **Williams JA, Pascual-Leone A, Fregni F** (2010) Interhemispheric modulation induced by cortical stimulation and motor training. Phys Ther 90: 398–410.
6. **Waters-Metenier S, Husain M, Wiestler T, Diedrichsen J** (2014) Bihemispheric transcranial direct current stimulation enhances effector-independent representations of motor synergy and sequence learning. J Neurosci 34: 1037–1050.
7. **Fregni F, Boggio PS, Mansur CG, Wagner T, Ferreira MJ, et al.** (2005) Transcranial direct current stimulation of the unaffected hemisphere in stroke patients. NeuroReport 16: 1551–1555.
8. **Hummel F, Celnik P, Giraux P, Floel A, Wu WH, et al.** (2005) Effects of non-invasive cortical stimulation on skilled motor function in chronic stroke. Brain, 128: 490–499.
9. **Boggio PS, Nunes A, Rigonatti SP, Nitsche MA, Pascual-Leone A, et al.** (2007) Repeated sessions of noninvasive brain DC stimulation is associated with motor function improvement in stroke patients. Restor Neurol Neurosci 25: 123–129.
10. **Mahmoudi H, Borhani Haghighi A, Petramfar P, Jahanshahi S, et al.** (2011) Transcranial direct current stimulation: electrode montage in stroke. Disabil Rehabil 33: 1383–1388.
11. **Zimerman M, Heise KF, Hoppe J, Cohen LG, Gerloff C, et al.** (2012) Modulation of training by single-session transcranial direct current stimulation to the intact motor cortex enhances motor skill acquisition of the paretic hand. Stroke 43: 2185–2191.

12. **Nitsche MA, Paulus W** (2000) Excitability changes induced in the human motor cortex by weak transcranial direct current stimulation. J Physiol (Lond) 527: 633–639.

13. **Hummel FC, Cohen LG** (2006) Non-invasive brain stimulation: a new strategy to improve neurorehabilitation after stroke? Lancet Neurol 5: 708–712.

14. **Kobayashi M, Théoret H, Pascual-Leone A** (2009) Suppression of ipsilateral motor cortex facilitates motor skill learning. Eur J Neurosci 29: 833–836.

15. **Kang EK, Paik NJ** (2011) Effect of a tDCS electrode montage on implicit motor sequence learning in healthy subjects. Exp Transl Stroke Med 3: 4.

16. **Mordillo-Mateos L, Turpin-Fenoll L, Millán-Pascual J, Núñez-Pérez N, Panyavin I, et al.** (2012) Effects of simultaneous bilateral tDCS of the human motor cortex. Brain Stimul 5: 214–222.

17. **Kidgell DJ, Goodwill AM, Frazer AK, Daly RM** (2013) Induction of cortical plasticity and improved motor performance following unilateral and bilateral transcranial direct current stimulation of the primary motor cortex. BMC Neurosci 14: 64.

18. **Lindenberg R, Nachtigall L, Meinzer M, Sieg MM, Flöel A** (2013) Differential effects of dual and unihemispheric motor cortex stimulation in older adults. J Neurosci, 33: 9176–9183.

19. **O'Shea J, Boudrias M-H, Staggg CJ, Bachtiar V, Kischka U, et al.** (2013) Predicting behavioral response to TDCS chronic motor stroke. NeuroImage 85: 924–933.

20. **Sehm B, Kipping J, Schäfer A, Villringer A, Ragert P** (2013) A comparison between uni- and bilateral tDCS effects on functional connectivity of the human motor cortex. Front Hum Neurosci, 7, 183. doi: 10.3389/fnhum.2013.00183

21. **Daskalakis ZJ, Christensen BK, Fitzgerald PB, Roshan L, Chen R** (2002) The mechanisms of interhemispheric inhibition in the human motor cortex. J Physiol (Lond) 543: 317–326.

22. **Kukaswadia S, Wagle-Shukla A, Morgante F, Gunraj C, Chen R** (2005) Interactions between long latency afferent inhibitions in the human motor cortex. J Physiol (Lond) 563: 915–924.

23. **Avanzino L, Teo JTH, Rothwell JC** (2007) Intracortical circuits modulate transcallosal inhibition in humans. J Physiol (Lond) 583: 99–114.

24. **Lee H, Gunraj C, Chen R** (2007) The effects of inhibitory and facilitatory intracortical circuits on interhemispheric inhibition in the human motor cortex. J Physiol (Lond) 580: 1021–1032.

25. **Lang N, Nitsche MA, Paulus W, Rothwell JC, Lemon RN** (2004) Effects of transcranial direct current stimulation over the human motor cortex on corticospinal and transcallosal excitability. Exp Brain Res 156: 439–443.

26. **Chen R, Yung D, Li JY** (2003) Organization of ipsilateral excitatory and inhibitory pathways in the human motor cortex. J Neurophysiol, 89: 1256–1264.

27. **Gilio F, Rizzo V, Siebner HR, Rothwell JC** (2003) Effects on the right motor hand-area excitability produced by low-frequency rTMS over human contralateral homologous cortex. J Physiol (Lond) 551: 563–573.

28. **Catsman-Berrevoets CE, Lemon RN, Verburgh CA, Bentivoglio M, Kuypers HG** (1980) Absence of callosal collaterals derived from rat corticospinal neurons. A study using fluorescent retrograde tracing and electrophysiological techniques. Exp Brain Res 39: 433–440.

29. **Ferbert A, Priori A, Rothwell JC, Day BL, Colebatch JG, et al.** (1992) Interhemispheric inhibition of the human motor cortex. J Physiol (Lond) 453: 525–546.

30. **Perez MA, Cohen LG** (2008) Mechanisms underlying functional changes in the primary motor cortex ipsilateral to an active hand. J Neurosci 28: 5631–5640.

31. **Nelson AJ, Hoque T, Gunraj C, Ni Z, Chen R** (2009) Bi-directional interhemispheric inhibition during unimanual sustained contractions. BMC Neurosci 10, 31. doi: 10.1186/1471-2202-10-31

32. **Hinder MR, Schmidt MW, Garry MI, Summers JJ** (2010) Unilateral contractions modulate interhemispheric inhibition most strongly and most adaptively in the homologous muscle of the contralateral limb. Exp Brain Res 205: 423–433.

33. **Nitsche MA, Paulus W** (2001) Sustained excitability elevations induced by transcranial DC motor cortex stimulation in humans. Neurol 57: 1899–1901.

34. **Nitsche MA, Nische MS, Klein CC, Tergau F, Rothwell JC, et al.** (2003) Level of action of cathodal DC polarisation induced inhibition of the human motor cortex. Clin Neurophysiol 114: 600–604.

35. **Trompetto C, Buccolieri A, Marchese R, Marinelli L, Michelozzi G, et al.** (2003) Impairment of transcallosal inhibition in patients with corticobasal degeneration. Clin Neurophysiol 114: 2181–2187.

36. **Tsutsumi R, Shirota Y, Ohminami S, Terao Y, Ugawa Y, et al.** (2012) Conditioning intensity-dependent interaction between short-latency interhemispheric inhibition and short-latency afferent inhibition. J Neurophysiol 108: 1130–1137.

37. **Tazoe T, Sasada S, Sakamoto M, Komiyama T** (2013) Modulation of interhemispheric interactions across symmetric and asymmetric bimanual force regulations. Eur J Neurosci, 37: 96–104.

38. **Nitsche MA, Seeber A, Frommann K, Klein CC, Rochford C, et al.** (2005) Modulating parameters of excitability during and after transcranial direct current stimulation of the human motor cortex. J Physiol (Lond) 568: 291–303.

39. **Scelzo E, Giannicola G, Rosa M, Ciocca M, Ardolino G, et al.** (2011) Increased short latency afferent inhibition after anodal transcranial direct current stimulation. Neurosci Lett 498: 167–170.

40. **Tremblay S., Beaulé V, Lepage JF, Théoret H** (2013) Anodal transcranial direct current stimulation modulates GABAB-related intracortical inhibition in the M1 of healthy individuals. NeuroReport 24, 46–50.

41. **Netz J, Ziemann U, Hömberg V** (1995) Hemispheric asymmetry of transcallosal inhibition in man. Exp Brain Res 104: 527–533.

42. **Bäumer T, Dammann E, Bock F, Klöppel S, Siebner HR, et al.** (2007) Laterality of interhemispheric inhibition depends on handedness. Exp Brain Res 180: 195–203.

43. **Pal PK, Hanajima R, Gunraj CA, Li JY, Wagle-Shukla A, et al.** (2005) Effect of low-frequency repetitive transcranial magnetic stimulation on interhemispheric inhibition. J Neurophysiol 94: 1668–1675.

44. **Di Lazzaro V, Pilato F, Dileone M, Profice P, Oliviero A, et al.** (2008) The physiological basis of the effects of intermittent theta burst stimulation of the human motor cortex. J Physiol (Lond) 586: 3871–3879.

45. **Suppa A, Ortu E, Zafar N, Deriu F, Paulus W, et al.** (2008) Theta burst stimulation induces after-effects on contralateral primary motor cortex excitability in humans. J Physiol (Lond) 586: 4489–4500.

46. **Shin H-W, Sohn YH** (2011) Interhemispheric transfer of paired associative stimulation-induced plasticity in the human motor cortex. NeurReport 22: 166–170.

47. **Tsutsumi R, Hanajima R, Terao Y, Shirota Y, Ohminami S, et al.** (2013) Effects of the motor cortical quadripulse transcranial magnetic stimulation (QPS) on the contralateral motor cortex and interhemispheric interactions. J Neurophysiol 111: 26–35.

48. **Di Lazzaro V, Manganelli F, Dileone M, Notturno F, Esposito M, et al.** (2012) The effects of prolonged cathodal direct current stimulation on the excitability and inhibitory circuits of the ipsilateral and contralateral motor cortex. J Neural Transm 119: 1499–1506.

49. **Kim DY, Lim JY, Kang EK, You DS, Oh MK, et al.** (2010) Effect of transcranial direct current stimulation on motor recovery in patients with subacute stroke. Am J Phys Med Rehabil 89: 879–886.

50. **Duque J, Murase N, Celnik P, Hummel F, Harris-Love M, et al.** (2007) Intermanual differences in movement-related interhemispheric inhibition. J Cogn Neurosci 19: 204–213.

51. **Tazoe T, Perez MA** (2013) Speed-dependent contribution of callosal pathways to ipsilateral movements. J Neurosci 33: 16178–16188.

52. **Batsikadze G, Moliadze V, Paulus W, Kuo MF, Nitsche MA** (2013) Partially non-linear stimulation intensity-dependent effects of direct current stimulation on motor cortex excitability in humans. J Physiol (Lond) 591: 1987–2000.

53. **Roche N, Lackmy A, Achache V, Bussel B, Katz R** (2009) Impact of transcranial direct current stimulation on spinal network excitability in humans. J Physiol (Lond) 587: 5653–5664.

54. **Roche N, Lackmy A, Achache V, Bussel B, Katz R** (2012) Effect of anodal tDCS on lumber propirospinal system in healthy subjects. Clin Neurophysiol 123: 1027–1034.